

Construction of a Full-Length Prototype of the BESIII Drift Chamber and On-Detector Test for the BESIII Drift Chamber Electronics

QIN Zhong-Hua^{1,2;1)} YAN Zhi-Kang^{1,3} CHEN Yuan-Bo¹ WU Ling-Hui^{1,2} LIU Jian-Bei^{1,2} CHEN Chang¹
XU Mei-Hang¹ WANG Lan¹ MA Xiao-Yan¹ JIN Yan¹ LIU Rong-Guang¹ TANG Xiao¹
ZHANG Gui-Fang¹ ZHU Qi-Ming¹ SHENG Hua-Yi¹ ZHU Ke-Jun¹

1 (Institute of High Energy Physics, CAS, Beijing 100049, China)

2 (Graduate University of Chinese Academy of Sciences, Beijing 100049, China)

3 (Micro-Electronics Laboratory, Department of Physics, Hunan University, Changsha 410082, China)

Abstract A full-length prototype of the BESIII drift chamber was built. The experience gained on gas sealing, high voltage supply and front-end electronics installation should be greatly beneficial to the successful construction of the BESIII drift chamber. An on-detector test of the BESIII drift chamber electronics was carried out with the constructed prototype chamber. The noise performance, drift time and charge measurements, and electronics gains were examined specifically. The final test results indicate that the electronics have a good performance and can satisfy their design requirements.

Key words BESIII drift chamber, full-length prototype, electronics

1 Introduction

The BESIII experiment^[1] at the upgrading Beijing Electron Positron Collider (BEPC II, $L \sim 10^{33} \text{cm}^{-2} \cdot \text{s}^{-1} @ E_{\text{cm}} = 3.78 \text{GeV}$)^[2] is designed with the main goals of high-precision measurements and search for new physics in the τ -charm energy region. To meet the requirements of the physics goals on BESIII, the central tracking system must provide good efficiency, high momentum resolution, good dE/dx resolution and excellent adaptability for high event rate, which are achieved by using a small-cell, low-material drift chamber filled with helium-based gases. In addition, the new electronics, based on pipeline design with zero data suppression, is used for the BESIII drift chamber readout.

In order to test the physics design of the BESIII drift chamber, to obtain experience for the construc-

tion of the actual chamber, to determine the operating parameters of the BESIII drift chamber electronics and to test its performance, a full-length prototype was built and a test was carried out with cosmic rays and accelerator beams.

2 Construction of the full-length prototype

2.1 Mechanical structure

The full-length prototype imitates a section of the BESIII drift chamber, and it is 2.2m long, 0.5m wide and 0.4m high. The overall view of the prototype is shown in Fig. 1. The mechanical structure of the prototype is composed of two endplates, four lateral surfaces and two groups of shielding elements. The two endplates, assembled via four aluminum rods, are made of aluminum with a thickness of 25mm. The lateral surfaces of the prototype, providing such

Received 16 June 2006

1) E-mail: qinzh@mail.ihep.ac.cn

functions as gas sealing and electric shielding, consist of four aluminum plates of 3mm thick. In order to protect and shield the front-end electronics, two groups of shielding elements, made up of several aluminum plates, are mounted on the endplates. A total of 158 gold-plated tungsten (3% Re) sense wires, 25 μm in diameter, and 572 gold-plated aluminum field wires, 110 μm in diameter, are strung between the two endplates. These feedthroughs with copper and aluminum crimp pins, designed for the BESIII drift chamber, are crimped manually to fix the sense wires and field wires, respectively.

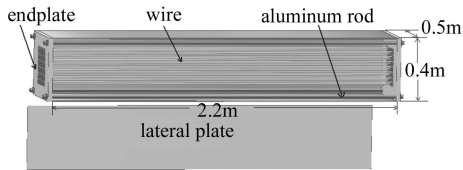


Fig. 1. Overall view of the full-length prototype (the two groups of shielding elements mounted on endplates are not shown).

2.2 Cell structure and wire layer arrangement

The full-length prototype adopts a small cell structure with the nominal half-cell width of 8.1mm, according to the cell design of the BESIII drift chamber. The individual drift cell is nearly square, with one sense wire in the center surrounded by eight field wires that are shared by the adjacent cells. A total of 158 drift cells, are arranged in 14 concentric sense layers, as shown in Fig. 2. The layers consist of two boundary layers (layer 1 and layer 14) and three

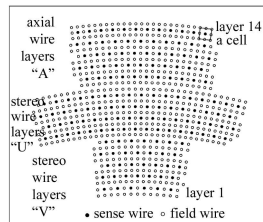


Fig. 2. Cell structure and wire layers arrangement of the full-length prototype (a view along z direction at the prototype center plane: $z=0$).

super-layers including one axial super-layer (layer 10 to 13) and two small-angle stereo super-layers (U and V, layer 2 to 9) alternating in stereo angle to implement the longitudinal measurements. The neigh-

boring layers in the same super-layer are staggered by half a cell, to resolve left-right ambiguity. In order to reduce the left-right asymmetry of the $x-t$ relations in the boundary layers, an additional field wire layer with the number of wires corresponding to the larger radius super-layer, is arranged between the axial super-layer and the stereo super-layer^[3].

2.3 Wire stringing, measurements of wire tension and leak current

The wires were strung inside a class 10000 clean room to prevent possible contaminations^[4]. To reduce the complexity, wire stringing was done horizontally. The mechanical tension of sense wires and field wires are, 52 and 172g, respectively, corresponding to an average gravitational sag of 102 μm at the center. Two semiautomatic measurement instruments, designed for the BESIII drift chamber, were used to measure the wire tensions and leak current of the prototype with the precision, 0.1g and 0.1nA, respectively. The measurement results show that the wire stringing is satisfactory and the instruments work well. The maximum difference of wire tensions is below 20%, especially, for these wires in the same layer, and the difference is controlled below 10% since the $x-t$ relation is determined layer by layer. Such requirements on wire tensions turn out to be acceptable since a good spatial resolution has been obtained in the beam test of the full-length prototype. And, the leak current of each cell is less than 2nA, which is small enough to have a negligible contribution to the noise.

2.4 Chamber sealing and gas leakage test

Many gas leak paths are possible because the prototype is assembled with several separate elements. We used different sealants and sealing measures for the different leak paths. There are four most possible leak paths in the chamber. First, the gaps between the endplates and the insulating bushes of feedthroughs are sealed with a silicone rubber compound, ShinEtsu RTV(KE45W). Second, the gaps between the copper tubes and the inner tubes of feedthroughs and that between the inner tubes and wires are sealed with an adhesive Loctite 609 due to its good flow and infiltration qualities. Third,

the main leak paths, between the lateral plates and the endplates, are sealed with ShinEtsu RTV with some latex strips filled in the gaps firstly. Last, all the screws are sealed with Loctite 290, which is also thought to have a good infiltration performance.

The procedures, used to make the gas leak test, are identical to those that have been used for the other drift chamber leak-down tests. We filled the chamber to about 10 times operating pressure with the pure helium, and then observed the decrease in pressure due to the leakage of the gas. Even for a chamber with no leaks, an increase in the atmospheric pressure or a decrease in gas temperature would appear to be a leak, so the influences due to the fluctuations of environment conditions must be considered in the measurement. The gas leak rate of the prototype is quite small, with 0.02% of the chamber volume per hour. The result indicates that the performance of sealants is good and the measures for sealing are reliable, which provide important preferences to the gas sealing of the BESIII drift chamber and its gas leak test.

2.5 Gas, HV system and front-end electronics installation

The operating gas of the prototype, is a helium-based gas mixture of Helium / C_3H_8 (60/40), with a flow rate corresponding to about one volume change per day. The gas system is running in open mode with an operating pressure slightly above the atmospheric pressure, and a well-calibrated mass flow meter is used to set and monitor the gas ratio and gas flow rate.

The method of high voltage power supply for the BESIII drift chamber was tested in the prototype experiment^[5]. A positive high voltage (about 2200V), offered by a remotely controlled high-voltage power supply, is connected to a distribution board which is composed of separating cards. And then, the high voltage is fanned out to several channels from the distribution card. Finally, it is connected to a high-voltage board and applied to the wires through a short wire. A total of 18 different high voltage settings are used in the prototype test, with 14 supplied to the sense wires and the other 4 supplied to the field

wires in the boundary layers to reduce the left-right asymmetry of the $x-t$ relation^[6]. The test results indicate that the HV system works successfully and with a very small noise.

The front-end electronics primarily consists of a preamplifier board and a high-voltage board mentioned above, which are arranged in the same printed circuit board and separated by a 1000pF capacitor and a 5M Ω resistor to simplify the design. The installation of front-end electronics is a key point to improve the performance and stability of the whole system. A good contact is achieved by directly mounting the front-end electronics on the endplates of the prototype and connecting it to the sense wires through well-designed connectors. Due to space limitation, the front-end electronics is distributed on both endplates with an odd-even layer staggering. The experience gained in the process is very useful for the installation of the actual drift chamber.

3 On-detector test for the BESIII drift chamber electronics

The BESIII drift chamber electronics were tested with the full-length prototype using cosmic rays and accelerator beams. After completing a preparatory cosmic ray test, a beam test was carried out at the E3 beam line at IHEP. The measures used to reduce noise, the performances of drift time and charge measurements, and the determination of electronics gains are discussed below in detail.

3.1 Description of the electronics

A standard electronics system, designed for the BESIII drift chamber, is used to process the signals of the prototype chamber^[1], primarily composed of the current-sensitive preamplifiers and the MQT modules. Since both the charge and time measurements are required for each signal, a trans-impedance type preamplifier is adopted so as to preserve the time information carried by the signal's rising edge. And, the MQT module integrates many functions such as post-amplification, shaping, discrimination, charge measurement and time measurement. Of these, the charge measurement adopts a numerical integration method based on a flash ADC (FADC) with 10 bit

resolution and 40MHz sampling, the charge value is extracted through successively digitizing the input analog signal and then integrating these digitized data. And, the arrival time of hit signal with respect to t_0 (the moment of particles passing through the chamber) is measured by the time measurement circuitry through a coarse time counter, a trigger counter and an external 40MHz clock. A total of 23 preamplifiers, each reading 8 sense wires, and 6 MQT modules, each containing 32 channels, were equipped in the cosmic ray test and beam test.

3.2 Noise reduction

A low noise level is necessitated for the electronics system due to the very small signal (about several μA) produced by the avalanche. The grounding and shielding, which are essential for the performance and stability of the whole system^[7], were developed to reduce noise in the cosmic ray test and beam test. In our case, the most critical points are good ground connections from the prototype to the preamplifier and from the preamplifier to the MQT module, and that is achieved by directly connecting the shields of cables, which deliver signals from preamplifiers to MQT modules, and to endplates of the prototype. In this way, the same ground potential is obtained to the detector and its electronics so as to eliminate the ground loops, and thus to suppress noise. In addition, shielding of the test chamber and its front-end electronics turns out to be another effective way to suppress noise by preventing space electromagnetic field interferences. At the beginning of the beam test, the noise, converted to the equivalent input current of the preamplifier, is up to about $5\mu\text{A}$, which is almost at the level of the signal current. As shown in Fig. 3(a), the system cannot work with a low electronics threshold aimed to improve the precision of timing so as to improve spatial resolution, due to a very high noise hit rate for almost all the cells. After a careful treatment of the grounding and shielding mentioned above, the system noise drops to below $0.4\mu\text{A}$, which is low enough that a clear track can be seen in Fig. 3(b). Such ways to reduce noise in the beam test will be applied to the assembling of the BESIII drift chamber.

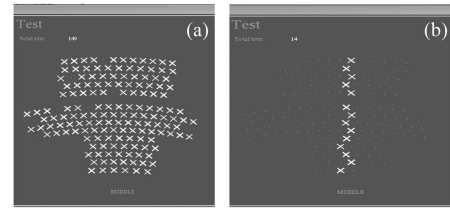


Fig. 3. On-line display for hits, the cell hit by a charged particle is marked with a “x”.

3.3 Test for drift time measurement

The drift time is accurately measured relying on a search window and a trigger latency in the MQT module. The main points are to open the search window with a width equal to or slightly greater than the maximum drift time and to set the trigger latency correctly so that the drift time to be measured is covered within this window. At the start of the cosmic-ray test, the search window was set at $2.5\mu\text{s}$, as shown in Fig. 4(a), which was too wide and led to a significant increase in noise, DAQ data stream and electronics dead-time. With many adjustments, the width of the search window was reduced to 600ns , and the data became much better as shown in Fig. 4(b). Also, the trigger latency was set at $6.4\mu\text{s}$ strictly as in the preliminary design^[1].

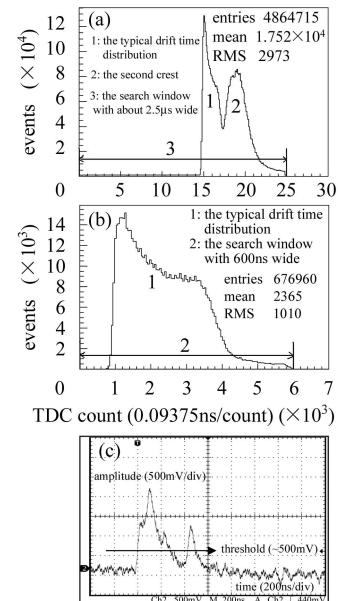


Fig. 4. (a) The drift time spectrum with a search window of $2.5\mu\text{s}$; (b) The drift time spectrum with a search window of 600ns ; (c) A signal observed before the discriminator of MQT with an oscilloscope. The electronics threshold is set at about 500mV typically, corresponding to about $0.36\mu\text{A}$ if converted to the sense wire current.

As shown in Fig. 4(a), it is noticeable that there is a secondary crest marked with No.2, compared to the typical drift time distribution marked with No.1. To understand this, we observed the output waveforms of preamplifiers and found that most signals had two crests with the width of 300—400ns and amplitude over the preset electronics threshold, as shown in Fig. 4(c). Hence, two different time values were measured to the same cell hit by charged particles and the secondary crest appeared. To prove this explanation, we filled the spectrum just using the first measured time (a smaller one). As a result, the secondary crest disappeared, as shown in Fig. 4(b). To reduce the amounts of DAQ data, the secondary measured time should be removed because we are only interested in the first time, which corresponds to the earliest arrival time of ionization electrons.

3.4 Test for charge measurement

The charge measurement adopts a scheme based on FADC and extracts the charge value through a numerical integration. So, the integration width should be set reasonably according to the shaped signal width to ensure the integrity of measured charges as well as to reduce the probability of signal pileup and noise picking up. We tested the integration width with the cosmic rays. Fig. 5(a) shows the charge spectrum with an integration width of $0.8\mu\text{s}$ and Fig. 5(b) shows that with an integration width of $1.5\mu\text{s}$.

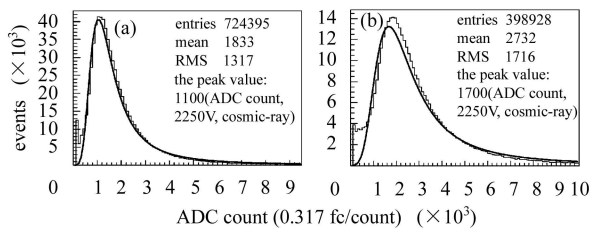


Fig. 5. (a) The charge spectrum with an integral width of $0.8\mu\text{s}$. The peak value is 1100 ADC counts; (b) The charge spectrum with an integral width of $1.5\mu\text{s}$. The peak value is 1700 ADC counts.

The large difference between the measured charges (i.e. the peak value, extracted from a well-known landau fitting of the charge spectrum) indicates that a $1.5\mu\text{s}$ integration width is necessary. The cases with a width above $1.5\mu\text{s}$ are also tested, with no significant difference found compared with the case in Fig. 5(b).

Since the shaped width of a signal has been determined to be about $1.3\mu\text{s}$, a slightly larger width of $1.5\mu\text{s}$ is a reasonable choice.

3.5 Determination of charge measurement gains

The amplitude of signals is limited due to a 2V dynamic range of FADCs. Since the preamplifier gain has been determined to be $\pm 12\text{mV}/\mu\text{A}$, a suitable post-amplification for signals should be considered to meet the requirement of FADCs. Taking into account the larger signals due to larger energy loss produced by lower momentum particles, the $0.5\text{GeV}/c$ protons are used to determine the charge measurement gains utilizing a waveform sampling technique, by which the signal waveforms are kept, thus the amplitude of signals can be measured easily. In this way, the post-amplifier gain is chosen as ~ 1.5 , so the total gains for charge measurement are $\sim 36\text{mV}/\mu\text{A}$. In this case, the number of signals with amplitude above 2V is less than 5%, which is an acceptable level for particle identification.

3.6 Performance of the electronics

In order to study the final performance of the prototype as well as the BESIII drift chamber electronics, we took data in test beam with changes of operating conditions such as high voltage, beam momentum and electronics threshold after completing all kinds of tests described above. Detailed results from the beam test have been obtained. Here only the primary results are presented, which reflect the final performances of the prototype and the electronics system. A good spatial resolution of $123\mu\text{m}$, averaged over the full drift distance, is extracted from

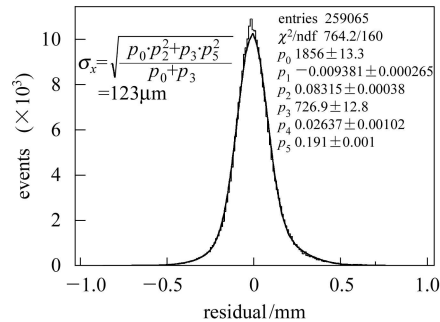


Fig. 6. The residual distribution with a dual-gaussian fitting (H.V.=2200V, $1\text{GeV}/c$ electron).

a dual-gaussian fitting to the residual distribution^[8] for high voltage setting of 2200V, as shown in Fig. 6. Also, a good dE/dx resolution better than 5% at 2150V with 40 samples, obtained through a combination of several events, is extracted from a gaussian fitting to the dE/dx distribution, as shown in Fig. 7.

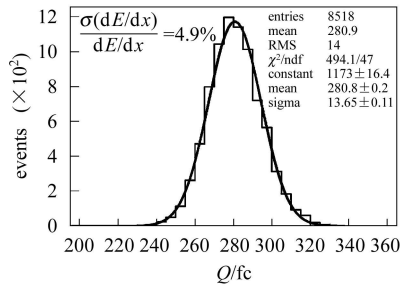


Fig. 7. The dE/dx resolution with a gaussian fitting (H.V.=2150V, 1GeV/c electron).

4 Conclusion

We designed and constructed a full-length prototype of the BESIII drift chamber, from which we accumulate much experience for the construction of the actual drift chamber. Some measures adopted for gas sealing, high-voltage supply and front-end electronics installation during the construction of the prototype provide important references to the BESIII drift chamber. We also carried out an on-detector test of the BESIII drift chamber electronics using the cosmic rays and accelerator beams. The final test results indicate that the electronics have excellent performances including a good noise performance, a high timing precision, a precise charge measurement, and a long-term stability, which well satisfy their design requirements. Detailed results from the cosmic ray test and beam test of the prototype will be published subsequently in other articles.

References

- BESIII Preliminary Design Report, 2004
- BEPCII Preliminary Design Report, 2002
- WU Ling-Hui et al. HEP & NP, 2005, **29**(5): 476—480 (in Chinese)
(伍灵慧等. 高能物理与核物理, 2005, **29**(5): 476—480)
- Andryakov A et al. Nucl. Instrum. Methods, 1998, **A404**: 248
- XU Mei-Hang et al. Nuclear Electronics & Detection Technology, 2006, **26**: 199 (in Chinese)
(徐美杭等. 核电子学与探测技术, 2006, **26**: 199)
- Peterson D et al. Nucl. Instrum. Methods, 2002, **A478**: 142
- Albrecht H et al. Nucl. Instrum. Methods, 2005, **A541**: 610
- LIU J B et al. Nucl. Instrum. Methods, 2006, **A557**: 436

BESIII 漂移室全长模型的建造及基于全长模型的 BESIII 漂移室电子学的测试

秦中华^{1,2;1)} 严志康^{1,3} 陈元柏¹ 伍灵慧^{1,2} 刘建北^{1,2} 陈昌¹ 徐美杭¹ 王岚¹ 马晓妍¹
金艳¹ 刘荣光¹ 唐晓¹ 张桂芳¹ 朱启明¹ 盛华义¹ 朱科军¹

1 (中国科学院高能物理研究所 北京 100049)

2 (中国科学院研究生院 北京 100049)

3 (湖南大学物理系微电子实验室 长沙 410082)

摘要 建造了 BESIII 漂移室全长模型. 在气体密封, 高压供给及前端电子学安装方面为 BESIII 漂移室的成功建造积累了经验. 另外, 在全长模型上对 BESIII 漂移室电子学进行了测试, 包括噪声, 漂移时间测量, 电荷测量, 以及电子学增益等方面. 测试的最终结果显示了 BESIII 漂移室电子学具有很好的性能, 能够满足它们的设计要求.

关键词 BESIII 漂移室 全长模型 电子学

2006 - 06 - 16 收稿

1) E-mail: qinzh@mail.ihep.ac.cn